



# An Integral-Equation Method Using Interstitial Currents Devoted to the Analysis of Multilayered Periodic Structures with Complex Inclusions

Nilufer A. Ozdemir, *Member, IEEE*, and Christophe Craeye, *Senior Member, IEEE*

**Abstract**—An efficient surface integral equation-based method is proposed for the analysis of electromagnetic scattering from multilayered media containing complex periodic inclusions. The proposed method defines equivalent currents at the interfaces between layers in order to eliminate the need to compute the layered medium Green's function. Hence, the background medium in a given layer can be treated as a homogeneous unbounded medium for which the computation of the Green's function for an infinite doubly periodic array is sufficient. The resulting method-of-moments interaction matrix has a block tridiagonal structure, which leads to computational complexity proportional to the number of layers for both matrix filling and solution. When all layers are identical, the filling time essentially reduces to that of a single layer, and the interaction matrix has a Toeplitz structure. Numerical results are provided for the reflectivity of multilayered periodic arrays of spherical silver core-silica shell nanoparticles, excited by a plane wave at optical frequencies. Comparisons with results obtained with an FDTD-based commercial software validate the accuracy and efficiency of the proposed method.

**Index Terms**—surface integral equations, method of moments, layered media, multilayered periodic structures, metamaterials, plasmonic nanostructures.

## I. INTRODUCTION

THE electromagnetic (EM) modeling and analysis of arbitrarily-shaped penetrable or non-penetrable objects embedded in layered media constitutes an active and important area of research. Such structures find applications at both microwave and optical frequencies such as microstrip antennas, microwave circuits, solar cells, lithography, and geophysical exploration. When the inclusions form a 2-D periodic lattice in each layer, such structures may be used as metamaterials, i.e. materials that may have, within certain frequency ranges, properties that cannot be found in nature [1]–[3]. Surface integral equation-based methods are advantageous for the numerical analysis of electromagnetic scattering from penetrable structures because, in those methods, the radiation condition is satisfied implicitly, and unknowns are limited to interfaces between piecewise homogeneous media. Among possible surface integral-equation formulations, the PMCHWT approach [4]–[6], which explicitly imposes the continuity of tangential electric and magnetic fields across interfaces, is widely employed [7]. The method-of-moments (MoM) [8] solution of the PMCHWT formulation has been

successfully applied to different periodic and non-periodic penetrable materials in a wide range of applications [9]–[15].

Traditionally, the integral equation-based numerical solution of this type of problems requires the computation of the layered medium Green's function in order to take into account the EM effect of layered media. However, obtaining the spatial-domain periodic Green's function for a layered medium from its analytically expressed spectral-domain counterpart requires the evaluation of Sommerfeld integrals or summations; the former for isolated sources and the latter for periodic sources. Such evaluations are computationally expensive processes due to the oscillatory and slowly decaying nature of the integrand or series [16]–[24]. The analysis of multilayered periodic structures using such an approach has two additional major drawbacks. First, the computational complexity of matrix filling is proportional to the square of the number of layers in the structure. Second, a new analysis is necessary every time a change is made in any layer.

The Generalized Scattering Matrix (GSM) [26] technique provides a solution to the latter two drawbacks. It describes the reflection and transmission properties of each layer by a scattering matrix, and it uses a cascading process to obtain a scattering matrix for the overall structure. To this end, every possible Floquet harmonic of the periodic incident field is considered, and the transmission and reflection coefficients for all Floquet harmonics are computed. The scattering matrix of the layered structure can then be obtained from the scattering matrices of the individual layers. In practice, the maximum order of Floquet harmonics depends on the period of the structures and on the thickness of the layers. Different numerical methods, such as the MoM [27] and the finite-difference time-domain (FDTD) method [28], have been employed to calculate the elements of the scattering matrix.

The present paper proposes an efficient surface integral equation method for the analysis of multilayered periodic objects which are either embedded in or located above layered media. The period will be assumed to be the same in each layer, but the host medium in different layers, their thicknesses and the inclusions they contain can be different. The proposed method, briefly introduced in [29], is based on surface equivalence used at two different levels. First, objects are analyzed via equivalent currents placed on the interfaces between piecewise homogeneous media. Second, when the objects are embedded in multiple layers, an equivalence plane, with equivalent electric and magnetic currents, is inserted at every interface between layers. Hence, the medium in a given layer

N. A. Ozdemir and C. Craeye are with the ICTEAM, Université Catholique de Louvain, Louvain-la-Neuve, B-1348 Belgium e-mail: {nilufer.ozdemir, christophe.craeye}@uclouvain.be.

Manuscript received August 10, 2014.

can be treated as a homogeneous unbounded medium, and the computation and tabulation of the doubly periodic Green's function is sufficient. Moreover, the global interaction matrix is Toeplitz when the background medium and the object remain identical in each layer. In the MoM solution, the interaction matrix for each layer is independent, and the global interaction matrix has a block tridiagonal form, inherited from the use of surface equivalence, which also allows the elimination of variables related to the complex inclusions. Here, contrary to the treatment of non-periodic complex objects [32]–[34], the exploitation of surface equivalence in layered periodic structures allows the reduction of equivalence surfaces to open surfaces with very small area, corresponding to the portion of interface between layers that is located within the unit cell. This leads to a very modest total number of unknowns in the final system of equations. The main advantage of the proposed method over the GSM method is that the whole formulation is based on a minimal set of types of quantities to be determined and of numerical tools to be used. Indeed, besides a traditional MoM solver for isolated penetrable bodies [7], the only building block needed is a code able to test electric and magnetic fields radiated by a 2-D periodic array of sources, decomposed into elementary basis functions [9]–[14]. From there, a reduced system of equations, involving only unknowns related to equivalent currents at the interfaces, is readily established. Those interfaces do not necessarily need to be planar; also, in case the inclusions are nearly touching the interfaces, it is in principle possible to refine the mesh on the interfaces in regions very close to the inclusions.

The remainder of this paper is organized as follows. Section II describes the details of the proposed numerical approach. Section III provides numerical results for the reflectivity of infinite layers made of doubly periodic arrays of spherical silver core-silica shell nanoparticles located above a silicon substrate. This structure corresponds to an interesting metamaterial with a minimum reflectivity for a wavelength near 400 nm [30]. The results are validated by comparison with numerical results obtained using the commercial software Lumerical [35] for arrangements comprising up to seven layers. Section IV outlines the main contributions and provides further perspectives for this approach.

## II. FORMULATION

The multi-layer structure is represented schematically in Fig. 1. There are  $N$  interfaces, numbered from 0 to  $N - 1$  bottom-to-top, and  $N - 1$  layers, numbered from 1 to  $N - 1$ , between the interfaces. Layer  $n$  is just beneath interface  $n$ , while homogeneous semi-infinite media above and below the layered structure are considered as layers 0 and  $N$ . Within the unit cell of the 2-D periodic structure, each layer 1 to  $N$  contains an *inclusion* that can consist of several disconnected objects. It is assumed that, in each layer, the objects are composed of piecewise homogeneous materials, and that the host medium is homogeneous. However, the host media composing different layers, the thicknesses of the layers, as well as the inclusions in successive layers, can be different. It is interesting to notice that, for the formulation given hereafter to be applicable, the interfaces do not need to be flat.

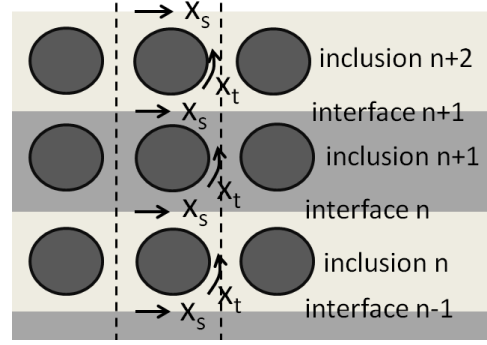


Fig. 1. Layered structure with inclusions, with numbering of layers and planar interfaces.

The formulation given hereafter relies on the surface equivalence principle. More precisely, the PMCHWT formulation [4]–[6], [7], sometimes also named “continuity formulation” [37], will be employed. In a nutshell, the PMCHWT approach defines equivalent electric and magnetic currents on each interface between homogeneous media. For simplicity, the formulation hereafter will be given for a homogeneous penetrable inclusion; the appendix briefly describes the extension to more complex inclusions. The equivalent electric and magnetic currents are  $\vec{J} = \hat{n} \times \vec{H}$  and  $\vec{M} = -\hat{n} \times \vec{E}$ , respectively;  $\hat{n}$  is the unit normal pointing outward the penetrable object, and  $\vec{H}$  and  $\vec{E}$  are the magnetic and electric fields. The equivalent currents are determined by explicitly ensuring the continuity of tangential electromagnetic fields across the surface of the object. That continuity also appears implicitly through the definition of opposite equivalent currents on both sides of the interface. As a convention, we will assume that the actual unknown currents are those just above the interfaces and just outside the inclusions (see Fig. 1). The continuity of tangential  $\vec{E}$  and  $\vec{H}$  fields will be imposed across both the interfaces and the boundaries of the inclusions. As will be explained hereafter, only the unknowns related to equivalent currents defined along the interfaces will appear in the final system of equations, which will be sparse.

The proposed formulation may be regarded as an extension of that described in [19], where the case of a single layer containing metallic inclusions is considered. As done in that paper, in general, the Green's function used to link sources and magnetic vector potential is the 2-D periodic scalar Green's function associated with the host material taken as an unbounded host medium. One exception to this rule must be considered: inside the inclusions, the link between equivalent currents and radiated fields is obtained using the scalar Green's function for an isolated source since the interior problem is not periodic. An important aspect of the proposed formulation is that the unknowns corresponding to the equivalent currents on the surface of the inclusions, which may sometimes have complex geometries, will be eliminated from the system of equations.

In order to alleviate the notation, the unknowns associated with the equivalent electric and magnetic currents defined on

a given interface are represented with a single vector  $\mathbf{x}$ :

$$\mathbf{x} = \begin{bmatrix} \mathbf{j} \\ \mathbf{m} \end{bmatrix} \quad (1)$$

where  $\mathbf{j}$  and  $\mathbf{m}$  are column vectors that respectively list the coefficients of equivalent electric and magnetic currents, with respect to the basis functions. Here, the same set of basis functions will be used to represent electric and magnetic currents. Besides, Garlekin testing will be used, in that the set of basis functions also corresponds to the set of testing functions.

The electric and magnetic fields tested by a set of testing functions defined on surface  $S_1$  and radiated by equivalent currents, described on surface  $S_2$  by a set of basis functions with coefficients  $\mathbf{x}_2$ , are obtained as  $\mathbf{y}_1 = \mathbf{Z} \mathbf{x}_2$ , with

$$\mathbf{Z} = \begin{bmatrix} \frac{\eta \mathbf{Z}^{EJ}}{j k} & \mathbf{Z}^{EM} \\ -\mathbf{Z}^{EM} & \frac{\mathbf{Z}^{EJ}}{j k \eta} \end{bmatrix} \quad (2)$$

where  $\eta$  and  $k$  are the impedance and wavenumber of the medium through which basis and testing functions interact, respectively. The  $\mathbf{Z}^{EJ}$  and  $\mathbf{Z}^{EM}$  matrix blocks are defined by:

$$Z_{k,l}^{EJ} = \int_{S_1} \int_{S_2} G(\vec{r}_1, \vec{r}_2) (k^2 \vec{F}_k(\vec{r}_2) \cdot \vec{F}_l(\vec{r}_1) - \nabla \cdot \vec{F}_k(\vec{r}_2) \nabla \cdot \vec{F}_l(\vec{r}_1)) dS_2 dS_1 \quad (3)$$

$$Z_{k,l}^{EM} = \int_{S_1} \int_{S_2} \nabla_1 G(\vec{r}_1, \vec{r}_2) \times \vec{F}_k(\vec{r}_1) \cdot \vec{F}_l(\vec{r}_2) dS_1 dS_2 \quad (4)$$

where  $\vec{F}_l$  and  $\vec{F}_k$  are the elementary basis function  $l$  and the testing function  $k$  on source domain  $S_2$  and observation domain  $S_1$ , respectively.  $G(\vec{r}_1, \vec{r}_2)$  is the scalar Green's function, which depends on the source and observation points  $\vec{r}_2$  and  $\vec{r}_1$  and on the properties of the material through which basis and testing functions are interacting.  $\nabla_1 G$  is the gradient of  $G$  with respect to the  $\vec{r}_1$  coordinates. Function  $G$  corresponds to the periodic Green's function in the medium of interest in all cases, except when the medium to be considered corresponds to the inner part of the inclusion. Fast calculations of the periodic Green's functions and of its gradient have been implemented as described in [11]. A non-exhaustive list of alternative formulations for the periodic Green's function is given in [37]. A more recent formulation is described in [24].

Hereafter, the  $\mathbf{Z}$  matrix is denoted by different symbols (from  $\mathbf{A}$  to  $\mathbf{E}$ ), depending on the pairs of surfaces  $S_1$  and  $S_2$  considered for the interactions:

- $\mathbf{Z} = \mathbf{A}$  when  $S_2$  is an interface and  $S_1$  is also an interface.
- $\mathbf{Z} = \mathbf{B}$  when  $S_2$  is boundary of inclusion and  $S_1$  is interface.
- $\mathbf{Z} = \mathbf{C}$  when  $S_2$  is interface and  $S_1$  is boundary of inclusion.
- $\mathbf{Z} = \mathbf{D}$  when  $S_2$  is boundary of inclusion and  $S_1$  is boundary of inclusion, in the host medium of the layer.
- $\mathbf{Z} = \mathbf{E}$  when  $S_2$  is boundary of inclusion and  $S_1$  is boundary of inclusion, in the medium inside the object (non-periodic Green's function used).

The two superscripts applied hereafter to those matrices will refer to the indices associated with surface  $S_1$  and  $S_2$ , respectively (see Fig. 1). When  $S_1$  and  $S_2$  both correspond to interface  $n$ , the interaction can take place through the host medium of layer  $n$  or layer  $n+1$ ; a subscript will then indicate which layer should be considered. The vectors of unknowns  $\mathbf{x}_s^n$  and  $\mathbf{x}_t^n$  will refer to the equivalent currents on interface  $n$  and on the boundary of the inclusion in layer  $n$ , respectively.

Using the above notation, and excluding the first and last interfaces (i.e.  $n \neq 0$  and  $n \neq N-1$ ), the continuity of tangential fields on interface  $n$  is imposed through:

$$\mathbf{A}_{n+1}^{n,n} \mathbf{x}_s^n - \mathbf{A}^{n,n+1} \mathbf{x}_s^{n+1} + \mathbf{B}^{n,n+1} \mathbf{x}_t^{n+1} = -\mathbf{A}_n^{n,n} \mathbf{x}_s^n + \mathbf{A}^{n,n-1} \mathbf{x}_s^{n-1} + \mathbf{B}^{n,n} \mathbf{x}_t^n \quad (5)$$

The continuity of tangential fields on the boundary of the inclusion in layer  $n$  is imposed through:

$$\mathbf{C}^{n,n} \mathbf{x}_s^n + \mathbf{C}^{n,n-1} \mathbf{x}_s^{n-1} + \mathbf{D}^{n,n} \mathbf{x}_t^n = -\mathbf{E}^{n,n} \mathbf{x}_t^n \quad (6)$$

The unknowns  $\mathbf{x}_t$ , referring to equivalent currents on the inclusions, can be eliminated between (5) written for interface  $n$  and (6) written for the inclusions in layers  $n$  and  $n+1$ . A few straightforward algebraic transformations then yield:

$$\mathbf{A}_1^n \mathbf{x}_s^{n-1} + \mathbf{A}_2^n \mathbf{x}_s^n + \mathbf{A}_3^n \mathbf{x}_s^{n+1} = 0 \quad (7)$$

still for  $n \neq 0$  and  $n \neq N-1$ , and with the following matrices:

$$\mathbf{A}_1^n = -\mathbf{A}^{n,n-1} - \mathbf{B}^{n,n} \mathbf{F}^n \quad (8)$$

$$\mathbf{A}_2^n = \mathbf{A}_{n+1}^{n,n} + \mathbf{A}_n^{n,n} + \mathbf{B}^{n,n+1} \mathbf{F}^{n+1} - \mathbf{B}^{n,n} \mathbf{G}^n \quad (9)$$

$$\mathbf{A}_3^n = -\mathbf{A}^{n,n+1} + \mathbf{B}^{n,n+1} \mathbf{G}^{n+1} \quad (10)$$

and the following definitions

$$\mathbf{F}^n = \mathbf{Y}^n \mathbf{C}^{n,n-1} \quad (11)$$

$$\mathbf{G}^n = \mathbf{Y}^n \mathbf{C}^{n,n} \quad (12)$$

$$\mathbf{Y}^n = -[\mathbf{E}^{n,n} + \mathbf{D}^{n,n}]^{-1} \quad (13)$$

Section III will show results for the case where inclusions are made of core-shell nanoparticles, for which (6) needs to be generalized as explained in the appendix.

The special cases of  $n = 0$  and  $n = N-1$  can be treated by setting  $\mathbf{A}^{0,-1} = 0$ ,  $\mathbf{B}^{0,0} = 0$ ,  $\mathbf{A}^{N-1,N} = 0$  and  $\mathbf{B}^{N-1,N} = 0$ , in order to avoid contributions from non-existing boundaries. First, quite expectedly, this leads to  $\mathbf{A}_1^0 = 0$  and  $\mathbf{A}_3^{N-1} = 0$ . Second, this also leads to

$$\mathbf{A}_2^0 = \mathbf{A}_1^{0,0} + \mathbf{A}_0^{0,0} + \mathbf{B}^{0,1} \mathbf{F}^1 \quad (14)$$

$$\mathbf{A}_2^{N-1} = \mathbf{A}_N^{N-1,N-1} + \mathbf{A}_{N-1}^{N-1,N-1} - \mathbf{B}^{N-1,N-1} \mathbf{G}^{N-1} \quad (15)$$

while  $\mathbf{A}_3^0$  and  $\mathbf{A}_1^{N-1}$  can be obtained from (10) and (8), respectively. The illumination from above only affects the condition to be satisfied at interface  $N-1$ , for which an additional term  $\mathbf{e}$  appears in the left hand side in (5). The vector  $\mathbf{e}$  is the tested incident field:

$$\mathbf{e} = \begin{bmatrix} \mathbf{t}^e \\ \mathbf{t}^h \end{bmatrix} \quad (16)$$

with

$$\mathbf{t}^e(k) = \int_S \vec{F}_k \cdot \vec{E}^{inc} dS \quad (17)$$

where  $\vec{E}^{inc}$  is the incident electric field and  $\vec{F}_k$  is the  $k$ -th basis function defined on interface  $n = N - 1$ . A similar expression, involving the incident magnetic field, is obtained for  $\vec{t}^h(k)$ .

Equations (8)-(10) and the special cases given above for layers 1 and  $N - 1$  define a block tridiagonal system of equations:

$$\begin{bmatrix} \mathbf{A}_2^0 & \mathbf{A}_3^0 & 0 & \dots & 0 \\ \mathbf{A}_1^1 & \mathbf{A}_2^1 & \mathbf{A}_3^1 & \dots & 0 \\ \vdots & & \ddots & & \vdots \\ 0 & \dots & 0 & \mathbf{A}_1^{N-1} & \mathbf{A}_2^{N-1} \end{bmatrix} \begin{bmatrix} \mathbf{x}_s^0 \\ \mathbf{x}_s^1 \\ \vdots \\ \mathbf{x}_s^{N-1} \end{bmatrix} = \begin{bmatrix} 0 \\ 0 \\ \vdots \\ -\mathbf{e} \end{bmatrix} \quad (18)$$

The sparse matrix results from the use of the surface equivalence principle, in that equivalent currents eliminate the direct interactions with inclusions and interfaces that are located beyond the immediately neighboring interfaces. Also, the elimination of the unknowns on the inclusions represent a huge time saving since complex inclusions may require a very large number of basis functions (and hence of unknowns) for an accurate representation of the fields on their boundaries. The latter can, however, always be obtained a posteriori from the equivalent currents on the interfaces, by isolating  $\mathbf{x}_t^n$  in (6). The unknowns describing the equivalent electric and magnetic currents on a given interface can be limited to a small number, typically ranging from 100 to 400, i.e. the number of entries in  $\mathbf{x}_s$  typically ranges from  $M=200$  to 800. Besides, if  $N$  is the number of interfaces, specialized solvers for block tridiagonal matrices can be used [40]; their complexity is simply proportional to  $N$ . Hence, the complexity of the solution process is of the order of  $M^3 N$ . Considering, for instance, a problem with 8 interfaces discretized with 256 basis functions (i.e. 512 unknowns per interface), independently from the complexity of the inclusions, will take the same time as the inversion of a square matrix of dimension 1024, i.e. a fraction of a second on a present-day desktop computer.

### III. NUMERICAL RESULTS

In this section, we validate the proposed numerical approach for a multilayered, infinite doubly periodic array of core-shell nanoparticles above a silicon substrate. This configuration has been studied in [30] in an attempt to realize low-index metamaterials using a newly developed self-assembling technology. The array is excited by an  $x$ -polarized plane wave propagating in the  $-z$  direction (see Fig. 2). The reflectivity of the array is obtained in the frequency range which corresponds to free-space wavelength  $\lambda_o$  ranging from 300 nm to 700 nm. The diameters of the silver core and silica shell are 26 nm and 82 nm, respectively. The periods of the array in  $x$  and  $y$  directions are both equal to 84 nm. The layers of arrays of core-shell nanoparticles in the  $z$  direction are separated by 2 nm. Fig. 2 illustrates the geometrical details of the array configuration. In this configuration, the lowest layer (i.e. layer 0) is taken as a semi-infinite space of silicon, the upper layer (i.e. layer  $N$ ) is made of air, and the host media of the  $N - 1$  intermediate layers are air. The refractive indices of silicon and fused silica are taken from [38] and [39], respectively. The refractive index of silver is based on Palik's measurements with a

correction term [42]. Those refractive indices are converted into complex relative permittivities assuming that the complex relative permeability is 1. Two different background media are considered and the core-shell inclusions have a certain level of complexity in both geometry and material composition. Hence, this structure forms an interesting example to validate the numerical method proposed here.

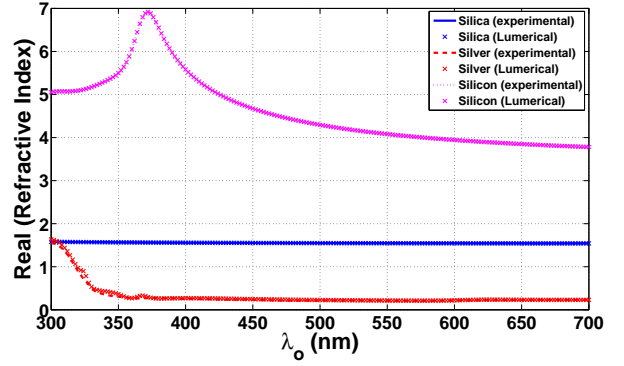


Fig. 3. Real part of refractive index of three materials used

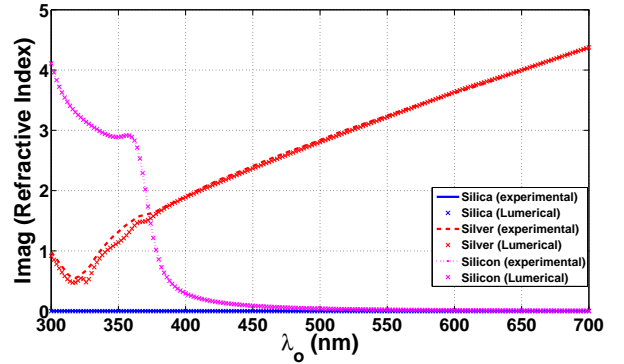


Fig. 4. Imaginary part of refractive index of three materials used

The surfaces of the silver core and of the silica shell are both discretized into 486 RWG [36] basis functions. The interface between silicon substrate and free space is discretized into 392 rooftop basis functions. The interface between the layers of particles in free space is discretized into 72 rooftop basis functions. The Lumerical FDTD solutions [35] software has been employed to produce the reference results. Lumerical has been used with the high mesh accuracy parameter and a minimum mesh step of 1 nm. A proper comparison between MoM and FDTD results requires a closer inspection of material parameters. Lumerical employs multi-coefficient models that multiply a set of basis functions to better fit dispersion profiles. For high accuracy frequency-domain outputs, this may not be sufficient to fit the experimental refractivity index data to the desired accuracy (e.g. with an error below 0.05). Hence, in this work, in order to obtain a better validation of accuracy of the MoM results, the highest number of coefficients has been used for the refractivity model used in Lumerical, and the corresponding model has been exploited in the MoM

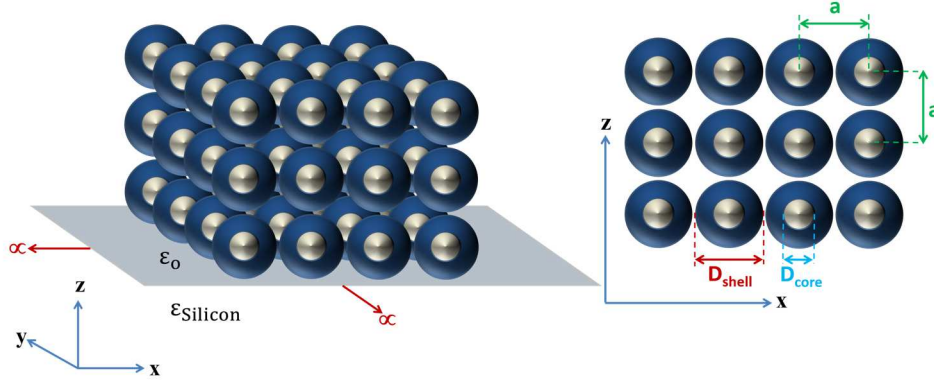


Fig. 2. The geometric details of the array configuration are given for the 3-layer, infinite doubly periodic array of core-shell nanoparticles.

simulations. Figures 3 and 4 show the real and imaginary parts of the refractive indices of silver, silicon, and silica, as from experiments [42], [38], [39], and as resulting from the Lumerical model referred to above.

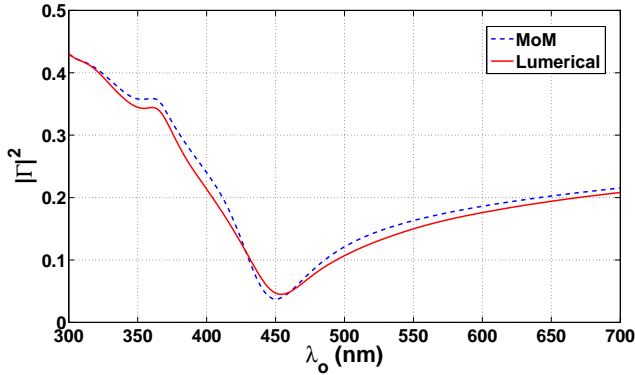


Fig. 5.a: Reflectivity for one layer.

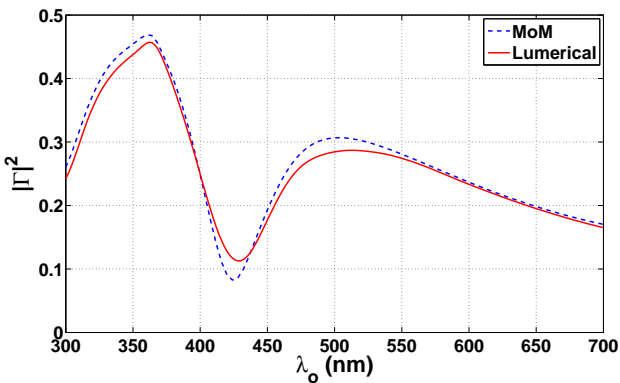


Fig. 5.b: Reflectivity for two layers.

Reflectivity results, i.e. the square-magnitude of the reflection coefficient, over the [300-700] nm wavelength range are shown in plots *a* to *g* of Fig. 5. A very good agreement between reflectivities obtained using the proposed approach and Lumerical is observed at all frequencies and for all

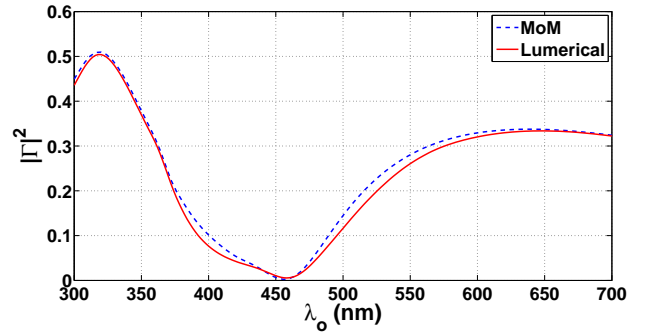


Fig. 5.c: Reflectivity for three layers.

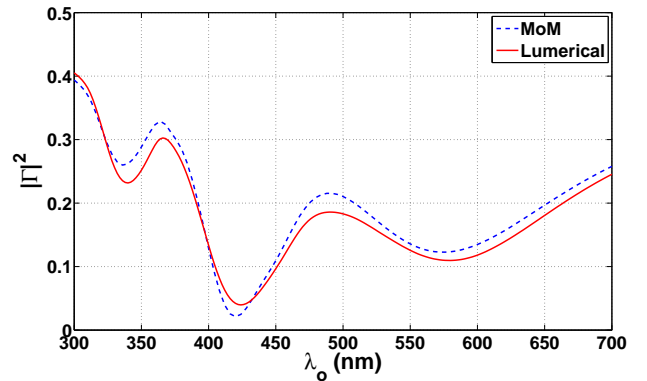


Fig. 5.d: Reflectivity for four layers.

numbers of layers. For a number of layers larger than three and for high reflectivity values (for  $|\Gamma|^2$  larger than about 0.15), the reflectivity predicted with our approach tends to be slightly higher than that predicted with Lumerical: a shift of the order of 0.02 is observed, although one does not observe a systematic shift, since there is virtually no shift in some sub-bands. Our investigations with both MoM and FDTD simulations did not allow us to determine which of both sets of results is most accurate.

Hereafter, computation times will be given for simulations



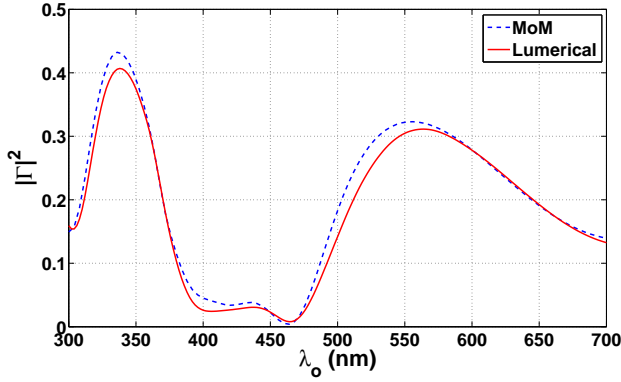


Fig. 5.e: Reflectivity for five layers.

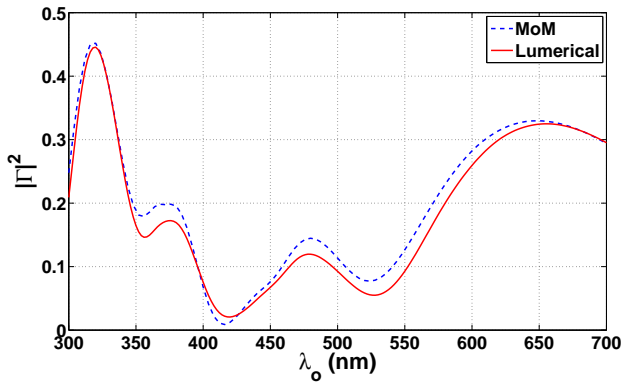


Fig. 5.f: Reflectivity for six layers.

carried out on a PC with Intel Core processor i74770K CPU with 3.5 GHz clock rate. On that computer, the Lumerical software uses 8 processors, while the MoM software uses only one, because the MoM code has not been parallelized yet. Hence, in order to compare, computation times will be converted to equivalent times for a single-processor operation, i.e. they will be multiplied by 8 for the FDTD computations

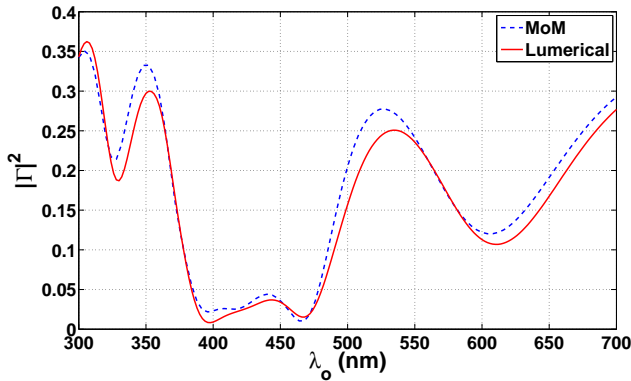


Fig. 5.g: Reflectivity for seven layers.

Fig. 5. Reflectivity for an increasing number of layers of silver-silica core-shell nano-particles above a silicon substrate. This MoM approach in dashed lines and Lumerical solution in solid lines.

TABLE I  
COMPUTATION TIMES IN SECONDS: MoM MATRIX COMPUTATIONS, ALL OTHER MoM COMPUTATIONS AND FDTD COMPUTATIONS ASSUMING ONLY ONE PROCESSOR

#	MoM matrices	MoM other	FDTD
1 layer	1060	66	17760
2 layers	1285	70	19200
3 layers	1285	79	19200
5 layers	1285	90	21220
7 layers	1285	98	26880

and left as is for the MoM calculations. One should note that this multiplication by 8 assumes a good parallelization scaling of the Lumerical software. The MoM approach can be strongly accelerated by exploiting interpolation of MoM matrices (i.e. the different types of  $\mathbf{Z}$  matrices referred to in Section II) versus frequency [41]. This leads to very important time savings, since -even for seven layers- the computation time is by far dominated by the filling of the MoM matrices. Here, over the frequency band of interest, the different  $\mathbf{Z}$  matrices are computed explicitly at only 11 of the 101 frequencies and second-order interpolation is used, without significant loss of accuracy at other frequencies (the maximum deviation for one layer in terms of reflectivity  $|r|^2$  is near 0.004, observed near the resonant peak of the silicon refractive index at 365 nm). The computation times are given in three columns in Table I: (i) MoM matrices obtained explicitly at 11 frequencies, (ii) all other computations involved in the MoM solution and (iii) FDTD calculations in terms of single-processor equivalent (8 times the solution time observed with parallel computation on 8 cores).

Taking into account that FDTD calculations have been carried out on eight cores, it can be seen that MoM calculations are faster by slightly more than one order of magnitude (more precisely by factors of 15.8, 14.2 and 19.4 for 1, 2 and 7 layers, respectively). Moreover, the MoM calculation time is by far dominated by the matrix filling time, which is never larger than the one needed for two layers; also, the total computation time for seven layers exceeds that for two layers by only 28 seconds, while considering the 101 frequencies at which reflectivity is computed. Finally, the MoM matrix filling computations for different frequencies could also be trivially distributed over several processors. The relatively large time involved in matrix filling underscores the relevance of further research in the acceleration of calculations of periodic Green's functions and MoM interactions between elementary basis functions. Regarding the latter, our implementation could be optimized in several respects.

#### IV. CONCLUSIONS

A new formulation has been presented for the simulation of scattering by multi-layered structures with periodic penetrable inclusions contained in each layer, and assuming common periods in the plane of the layers. The method requires a minimal set of calculation routines, corresponding to electric or magnetic-type interactions between basis and testing functions, using a 2-D periodic Green's function in unbounded homogeneous space. The principal characteristic of the method

is the introduction of interstitial equivalent currents at the interfaces, which allows the decoupling of non-adjacent layers. In this way, the use of Green's functions associated with multilayered media is avoided, the unknowns associated with the complex inclusions can be eliminated from the final system of equations; and the complexity grows only linearly with the number of layers.

Validating numerical results have been provided for the case of scattering by stacked layers of core-shell nano-particles placed above a silicon substrate. A very good agreement has been observed, as compared with results obtained with a commercial software based on FDTD, while computation times are shorter by a factor of the order of 16 for the MoM calculations. Given this efficient treatment of the multilayered aspect of the structures, it becomes clear that further research should focus on the acceleration of MoM matrix-filling techniques for the relatively fundamental problem of periodic structures in unbounded media. Further research also concerns implementations with non-planar interfaces, which may, for instance, be considered in the case of hexagonal arrangements, as well as the possibility of refining the mesh at interfaces, specifically in regions extremely close to the inclusions.

#### ACKNOWLEDGEMENT

This work has been funded by the EU METACHEM project and by the Belgian BESTCOM project and by the Belgian Interuniversity Attraction Poles Programme 7/23 BESTCOM.

#### APPENDIX

In the case where a secondary inclusion is embedded into a primary inclusion, as considered in Section III, where the silica inclusion contains a silver core, expression (6) needs to be generalized. Let us denote by  $\mathbf{x}_i^n$  the equivalent current on the outer boundary of the secondary inclusion, and by  $S_t$  and  $S_i$  the surfaces that enclose the primary and secondary inclusions, respectively. Then we can write:

$$\begin{aligned} \mathbf{C}^{n,n} \mathbf{x}_s^n + \mathbf{C}^{n,n-1} \mathbf{x}_s^{n-1} + \mathbf{D} \mathbf{x}_t^n &= -\mathbf{E} \mathbf{x}_t^n + \mathbf{M}_{t,i} \mathbf{x}_i^n \quad (19) \\ \mathbf{M}_{i,t} \mathbf{x}_t^n + \mathbf{M}_{i,i} \mathbf{x}_i^n &= -\mathbf{N} \mathbf{x}_i^n \quad (20) \end{aligned}$$

where  $\mathbf{M}_{a,b}$  is a  $\mathbf{Z}$ -type matrix standing for interaction, through the medium between  $S_t$  and  $S_i$ , between basis functions located on  $S_b$  and testing functions on surface  $S_a$ , where indices  $a$  and  $b$  can both correspond to either  $t$  or  $i$  indices. Matrix  $\mathbf{N}$  has the same definition as matrix  $\mathbf{E}$ , except that the surface is that of the secondary inclusion and that the medium considered is the one inside that inclusion. The other matrices have been defined in Section II. To alleviate notations, superscripts  $n, n$  have been removed from the matrices that were wearing them. Then, the current on the secondary inclusion can be eliminated between equations (19) and (20), to obtain an equation that has exactly the same form as (6), assuming a new definition for matrix  $\mathbf{E}$ .

#### REFERENCES

- [1] D.R. Smith, W. Vier, S. Nemat-Nasser, S. Schultz, "Composite medium with simultaneously negative permeability and permittivity," *Physical Review Lett.*, vol. 84, no. 18, pp. 4184-4187, 2000.
- [2] J.B. Pendry, "Negative refraction," *Contemporary Physics*, Princeton University Press, vol. 45, no. 3, pp. 191-202, 2004.
- [3] N. Engheta, R. Ziolkowski, *Metamaterials: Physics and Engineering Explorations*, Wiley and Sons, 2006.
- [4] J. Poggio and E. K. Miller, "Integral equation solution of three dimensional scattering problems," *Computer Techniques for Electromagnetics*, R. Mittra, ed., Pergamon, 1973.
- [5] Y. Chang and R. Harrington, "A surface formulation for characteristic modes of material bodies," *IEEE Trans. Antennas Propag.* vol. 25, pp. 789-795, 1977.
- [6] T. K. Wu and L. L. Tsai, "Scattering from arbitrarily-shaped lossy dielectric bodies of revolution," *Radio Sci.*, vol. 12, pp. 709-718, 1977.
- [7] S.M. Rao and D.R. Wilton, "E-Field, H-Field, and combined field solution for arbitrarily shaped three-dimensional dielectric bodies," *Electromagnetics*, vol. 10, no. 4, pp. 407-421, 1990.
- [8] R. F. Harrington, *Field Computation by Moment Method*, IEEE Press, 1993.
- [9] B.C. Usner, K. Sertel, and J.L. Volakis, "Doubly periodic volume-surface integral equation formulation for modelling metamaterials," *IET Microw. Antennas Propag.*, vol. 1, no. 1, pp. 150-157, Feb. 2007.
- [10] X. Dardenne and C. Craeye, "Method of moments simulation of infinitely periodic structures combining metal with connected dielectric objects," *IEEE Trans. Antennas Propag.*, vol. 56, no. 8, pp. 2372-2380, Aug. 2008.
- [11] N. Guérin, C. Craeye, X. Dardenne, "Accelerated computation of the free space Green's function gradient of infinite phased arrays of dipoles," *IEEE Trans. Antennas Propag.*, vol. 57, pp. 3430-3434, Oct. 2009.
- [12] B. Gallinet, A. M. Kern and O. J. F. Martin, "Accurate and versatile modeling of electromagnetic scattering on periodic nanostructures with a surface integral approach," *J. Opt. Soc. Am. A*, vol. 27, no. 10, pp. 2261-2271, Oct. 2010.
- [13] A. M. Kern and O. J. F. Martin, "Surface integral formulation for 3D simulations of plasmonic and high permittivity nanostructures," *J. Opt. Soc. Am. A*, vol. 26, no. 4, pp. 732-740, Apr. 2009.
- [14] J. Rivero, J. M. Taboada, L. Landesa, F. Obelleiro, and I. García-Tuñón, "Surface integral equation formulation for the analysis of left-handed metamaterials," *Opt. Express*, vol. 18, no. 15, pp. 15876-15886, Jul. 2010.
- [15] M. G. Araújo, J. M. Taboada, D. M. Solís, J. Rivero, L. Landesa, and F. Obelleiro, "Comparison of surface integral equation formulations for electromagnetic analysis of plasmonic nanoscatterers," *Opt. Express*, vol. 20, no. 8, pp. 9161-9171, Apr. 2012.
- [16] M. I. Aksun and R. Mittra, "Derivation of closed-form Green's functions for a general microstrip geometry," *IEEE Trans. Microw. Theory Tech.*, vol. 40, no. 11, pp. 2055-2062, Nov. 1992.
- [17] K. A. Michalski, "Extrapolation methods for Sommerfeld integral tails," *IEEE Trans. Antennas Propag.*, vol. 46, no. 10, pp. 1405-1418, Oct. 1998.
- [18] R. R. Boix, F. Mesa, and F. Medina, "Application of total least squares to the derivation of closed-form Green's functions for planar layered media," *IEEE Trans. Microw. Theory Tech.*, vol. 55, no. 2, pp. 268-280, Feb. 2007.
- [19] J. R. Mosig, "The weighted averages algorithm revisited," *IEEE Trans. Antennas Propag.*, vol. 60, no. 4, pp. 2011-2018, Apr. 2012.
- [20] M. M. Tajdini and H. Mosallaei, "Characterization of large array of plasmonic nanoparticles on layered substrate: dipole mode analysis integrated with complex image method," *Opt. Express*, vol. 19, no. 2, pp. 173-193, Mar. 2011.
- [21] Y. P. Chen, W. E. I. Sha, W. C. H. Choy, L. Jiang, and W. C. Chew, "Study on spontaneous emission in complex multilayered plasmonic system via surface integral equation approach with layered medium Green's function," *Opt. Express*, vol. 20, no. 18, pp. 20210-20221, Aug. 2012.
- [22] T. Eibert, J. Volakis, D. Wilton, and D. Jackson, "Hybrid FE/BI modeling of 3D Doubly periodic structures utilizing triangular prismatic elements and an MPIE formulation accelerated by the Ewald transformation," *IEEE Trans. Antennas Propag.*, vol. 47, no. 5, May 1999.
- [23] G. Valerio, P. Baccarelli, S. Paulotto, F. Frezza, and A. Galli, "Regularization of mixed-potential layered media Green's function for efficient interpolation procedures in planar periodic structures," *IEEE Trans. Antennas Propag.*, vol. 57, no. 1, pp. 122134, Jan. 2009.
- [24] V. Volski, G.A.E. Vandenbosch, "Quasi 3-D mixed potential integral equation formulation for periodic structures," *IEEE Trans. Antennas Propag.*, vol. 61, no. 4, pp. 2068-2076, Jan. 2009.



- [25] N. A. Ozdemir, C. Simovski, D. Morits and C. Craeye, "Efficient method of moments analysis of an infinite array of triangular nanoclusters in the optical frequency range," in *Int. Conf. on Electromagnetics in Advanced Applications Digest (ICEAA 2011)*, Torino, Italy, Sept. 12-16, 2011, pp. 359–362.
- [26] R. C. Hall, R. Mittra, and K. M. Mitzner, "Analysis of multilayered periodic structures using generalized scattering matrix theory," *IEEE Trans. Antennas Propag.*, vol. 36, no. 4, pp. 511–517, Apr. 1988.
- [27] A. I. Khali and M. B. Steer, "A generalized scattering matrix method using the method of moments for electromagnetic analysis of multilayered structures in waveguide," *IEEE Trans. Antennas Propag.*, vol. 47, no. 11, pp. 2151–2157, Nov. 1999.
- [28] K. ElMahgoub, F. Yang, and A. Z. Elsherbeni, "FDTD/GSM analysis of multilayered periodic structures with arbitrary skewed grid," *IEEE Trans. Antennas Propag.*, vol. 59, no.12, pp. 1133–1144, Dec. 2011.
- [29] N. A. Ozdemir, C. Craeye, K. Ehrhardt, and A. Aradian, "Efficient integral equation approach for metamaterials made of core-shell nanoparticles at optical frequencies," in *Proc. 7th European Conference on Antennas and Propagation (EUCAP 2013)*, Gothenburg, Sweden, Apr. 8-12, 2013, pp. 1840-1842.
- [30] L. Malassis, P. Massé, M. Tréguer-Delapierre, S. Mornet, P. Weisbecker, V. Kravets, A. Grigorenko, and P. Barois, "Bottom-up fabrication and optical characterization of dense films of meta-atoms made of core-shell plasmonic nanoparticles," *Langmuir*, vol. 29, no. 5, pp. 1551–1561, Jan. 2013.
- [31] N.A. Ozdemir and C. Craeye, "Efficient integral equation-based analysis of finite periodic structures in the optical frequency range," *Journ. Optical Soc. America*, vol. 30, no. 12, pp. 2510-2518, Dec. 2013.
- [32] A.M. van de Water, B.P. de Hon, M.C. van Beurden, and A.G. Tijhuis, "Linear embedding via Green's operators: a modelling technique for finite electromagnetic bandgap structures," *Phys. Rev. E*, vol. 72, no. 056704, pp. 111, 2005.
- [33] M.K. Li and W. C. Chew, "Wave-field interaction with complex structures using equivalence principle algorithm," *IEEE Trans. Antennas Propag.*, vol. 55, pp. 130-138, Jan 2007.
- [34] V. Lancellotti, B. P. de Hon, and A. G. Tijhuis, "An eigencurrent approach to the analysis of electrically large 3-D structures using linear embedding via Green's operators," *IEEE Trans. Antennas Propag.*, vol. 57, pp. 3575-3585, Nov. 2009.
- [35] LUMERICAL Solutions Inc., <https://www.lumerical.com/tcad-products/fdtd/>
- [36] S. Rao, D. Wilton, and A. Glisson, "Electromagnetic scattering by surfaces of arbitrary shape," *IEEE Trans. Antennas Propag.*, vol. 30, no. 3, pp. 409–418, Mar. 1982.
- [37] C. Craeye, X. Radu, A. Schuchinsky and F. Capolino, "Fundamentals of method of moments for artificial materials," in *Handbook of Artificial Materials*, Ed. F. Capolino, Taylor and Francis, June 2009.
- [38] SOPRA database <http://www.sopra-sa.com>.
- [39] M. Bass, C. DeCusatis, J. Enoch, V. Lakshminarayanan, G. Li, C. MacDonald, V. Mahajan, E. Van Stryland, *Handbook of Optics*, 3rd edition, Vol. 4. McGraw-Hill (2009).
- [40] W. Press, S. Teukolsky, W. Vetterling, B. Flannery, *Numerical recipes in C*, Third Edition, 1256 pp., Cambridge University Press, 2007.
- [41] E. Newman, "Generation of wide-band data from the method of moments by interpolating the impedance matrix [EM problems]," *IEEE Trans. Antennas Propag.*, vol. 36, no. 12, pp. 1820–1824, Dec. 1988.
- [42] E.D. Palik, *Handbook of Optical Constants of Solids*, Academic Press, 1991.